© 2016. Published by The Company of Biologists Ltd | Journal of Experimental Biology (2016) 219, 1214-1223 doi:10.1242/jeb.132282

RESEARCH ARTICLE

Development of endothermy and concomitant increases in cardiac and skeletal muscle mitochondrial respiration in the precocial Pekin duck (*Anas platyrhynchos domestica*)

Sarah K. G. Sirsat[1], Tushar S. Sirsat[1], Alan Faber[2], Allison Duquaine[1], Sarah Winnick[1], Paul R. Sotherland[2] and Edward M. Dzialowski[1,*]

ABSTRACT

Attaining endothermic homeothermy occurs at different times post-hatching in birds and is associated with maturation of metabolic and aerobic capacity. Simultaneous measurements at the organism, organ and cellular levels during the transition to endothermy reveal means by which this change in phenotype occurs. We examined development of endothermy in precocial Pekin ducks (*Anas platyrhynchos domestica*) by measuring whole-animal O_2 consumption ($\dot{V}_{O_2}$) as animals cooled from 35 to 15°C. We measured heart ventricle mass, an indicator of O_2 delivery capacity, and mitochondrial respiration in permeabilized skeletal and cardiac muscle to elucidate associated changes in mitochondrial capacities at the cellular level. We examined animals on day 24 of incubation through 7 days post-hatching. $\dot{V}_{O_2}$ of embryos decreased when cooling from 35 to 15°C; $\dot{V}_{O_2}$ of hatchlings, beginning on day 0 post-hatching, increased during cooling with a lower critical temperature of 32°C. Yolk-free body mass did not change between internal pipping and hatching, but the heart and thigh skeletal muscle grew at faster rates than the rest of the body as the animals transitioned from an externally pipped paranate to a hatchling. Large changes in oxidative phosphorylation capacity occurred during ontogeny in both thigh muscles, the primary site of shivering, and cardiac ventricles. Thus, increased metabolic capacity necessary to attain endothermy was associated with augmented metabolic capacity of the tissue and augmented increasing O_2 delivery capacity, both of which were attained rapidly at hatching.

KEY WORDS: Oxidative phosphorylation, Thermoregulation, Metabolism, Mitochondria, Cardiac muscle, Skeletal muscle, Avian

INTRODUCTION

Birds develop along a spectrum of functional maturity associated with endothermic capacity of the hatchling (Starck and Ricklefs, 1998). All bird embryos are ectothermic, relying on external sources of heat to remain homeothermic throughout incubation. Altricial species hatch featherless with very limited thermoregulatory capacity, and develop an endothermic phenotype while in the nest over a period of days to weeks (Olson, 1992). In contrast, precocial species hatch fully feathered and quickly develop endothermic thermoregulatory capacity (Whittow and Tazawa, 1991; Sirsat and Dzialowski, 2016).

[1]Developmental Integrative Biology Research Group, Department of Biological Science, 1155 Union Circle #305220, University of North Texas, Denton, TX 76203, USA. [2]Department of Biology, Kalamazoo College, Kalamazoo, MI 49008, USA.

*Author for correspondence (edzial@unt.edu)

Received 23 November 2015; Accepted 11 February 2016

A model for development of endothermy in precocial species proposes the following: development of endothermy is limited by oxygen delivery in late-stage embryos by eggshell O_2 gas conductance; after hatching, birds are no longer oxygen-limited, they are power-limited with heat-generating muscles exhibiting a limited metabolic capacity and varying ability to increase heat production depending on the extent of development (Whittow and Tazawa, 1991). Therefore, attaining an endothermic metabolic phenotype requires development of an aerobic capacity that can support energy demands during exposure to thermal challenges. This enhanced aerobic capacity must be met by high O_2 delivery via the respiratory and cardiovascular systems. During external pipping, the rigid eggshell surrounding the embryo prevents increasing pulmonary ventilation in response to environmental change, placing a limit on the capacity to increase O_2 delivery (Sirsat and Dzialowski, 2016). Minute ventilation increases at hatching and precocial Pekin ducks can respond to cooling by increasing ventilation (Sirsat and Dzialowski, 2016). Thus, a ventilation limit on the O_2 cascade appears to exist during the last stages of development in the egg. Limits imposed by the cardiovascular system and metabolic tissues in the O_2 cascade during this transition to endothermy, as suggested by Whittow and Tazawa (1991), have yet to be fully elucidated.

Because adult endotherms have a cardiac ventricle mass significantly larger than that of similar sized ectotherms, resulting in greater cardiac output and function (Driedzic et al., 1987; Hulbert and Else, 1989), birds transitioning from ectothermy (as embryos) to endothermy (as hatchlings) could experience a concomitant growth of the heart that outpaces growth of the body. Cardiac ventricles of white leghorn chickens (*Gallus gallus domesticus*) significantly increase in mass, with no change in yolk-free body mass, during the transition from external pipping to hatching (T. L. Killpack, A change of heart in birds: cardiac response to the onset of endothermy, Senior Thesis, Kalamazoo College, 2005). Furthermore, because the heart of an endotherm likely requires a greater oxidative phosphorylation (OXPHOS) capacity to provide the ATP necessary to function at a higher level than that of an ectotherm heart, oxidative capacities and number of mitochondria in endothermic hatchlings will likely be higher than that in ectothermic embryos and hatchlings. Little is known, however, about the ontogeny of cardiac mitochondrial function in bird hatchlings.

Birds rely heavily on shivering thermogenesis in skeletal muscles to produce the heat necessary to regulate body temperature under cold thermal stress. Shivering capacity develops rapidly in precocial species upon hatching, and the leg muscles, used for locomotion in precocial species at hatching, are a major site of shivering thermogenesis (Marjoniemi and Hohtola, 1999). Additionally, a number of precocial birds exhibit non-shivering thermogenesis, which can potentially contribute to regulating body temperature

Journal of Experimental Biology

Journal of Experimental Biology (2016) 219, 1214-1223 doi:10.1242/jeb.132282

List of symbols and abbreviations

CI	complex I
CII	complex II
EP	externally pipped
D0	day 0 post-hatching
D3	day 3 post-hatching
ETS	electron transport system
FCCP	carbonylcyanide *p*-trifluoromethoxy-phenylhydrazone
$F_{E_{O_2}}$	excurrent O_2 fraction of dry gas
$F_{I_{O_2}}$	incurrent O_2 fraction of dry gas
IP	internally pipped
$LEAK_N$	non-phosphorylating 'resting' mitochondrial respiration in the absence of adenylates
M_e	yolk-free embryo mass
M_h	heart mass
OXPHOS	oxidative phosphorylation
T_a	air temperature
$\dot{V}_I$	incurrent flow rate
$\dot{V}_{O_2}$	oxygen consumption rate

(Duchamp and Barre, 1993; Teulier et al., 2014). Metabolically demanding activities such as locomotion and thermogenesis rely on the aerobic capacity of skeletal muscles and associated mitochondrial bioenergetics. However, no studies have examined the ontogeny of skeletal mitochondrial function and *in situ* oxidative capacity in precocial species transitioning from the ectothermic phenotype in the egg to the endothermic phenotype in the hatchling.

We carried out this study to examine the ontogeny of endothermy and development of tissue level aerobic capacity in the Pekin duck (*Anas platyrhynchos domestica* Linnaeus), an excellent model for examining maturation of endothermy at the time of hatching (Sirsat and Dzialowski, 2016). We hypothesized that an increased endothermic and aerobic capacity should be associated with development of a relatively larger heart and an increase in mitochondrial respiration and the capacity for oxidative phosphorylation in skeletal and cardiac muscle. We characterized ontogeny of whole-animal oxygen consumption ($\dot{V}_{O_2}$) in response to cooling to assess when and how an endothermic phenotype develops in the Pekin duck. We also examined cardiac ventricle mass and mitochondrial respiration, in both skeletal and cardiac muscle, to reveal their developmental trajectories and to ascertain whether at any point they may limit an endothermic response to cooling.

MATERIALS AND METHODS

Animals

Pekin duck eggs were obtained from a commercial producer (Blanco Industries, McKinney, TX, USA) and incubated at 37.5°C and 60% relative humidity in an incubator (Model 1202, GQF Manufacturing, Savannah, GA, USA). Eggs were automatically turned along their polar axis every 4 h. Just prior to hatching, internally pipped eggs were moved into a clear Lyon incubator maintained at 37.5°C and 85% relative humidity. Time-lapse images of the eggs were taken every 30 min during the hatching process to determine time of hatching, which was then used to determine age of each hatchling during experimental use. Hatchlings were maintained in a Hatchrite incubator at 32°C with *ad libitum* access to water and food.

Metabolic rate

Metabolic rate of embryos and hatchlings was measured as oxygen consumption by flow-through respirometry during gradual cooling as in Sirsat and Dzialowski (2016). Animals were placed inside appropriately sized respirometry chambers (range 500 to 1000 ml), which were placed inside a programmable incubation chamber set to 37.5°C for embryos and 32°C for hatchlings. Animals acclimated for at least 60 min prior to cooling. Incubation chamber temperature was gradually decreased at a rate of 9.2°C h^{-1} until it reached 15°C. Gas containing 21% oxygen with nitrogen as the balance was pumped into the respirometry chambers at a known flow rate measured with a calibrated flow meter (Flowbar 1, Sable Systems, Las Vegas, NV, USA, calibrated with a soap bubble meter at STPD). A sample stream of the outflow gas was pulled by a pump (R1 flow controller, AEI Technologies, Pittsburgh, PA, USA) through a Nafion tubing drier surrounded by Drierite, Sodasorb and another Nafion tube drier for water and CO_2 removal before it was pulled through an O_2 analyzer (FC-1B, Sable Systems). Data were recorded with LabChart 7 and a PowerLab 8SP (ADInstruments, Colorado Springs, CO, USA). Sampling of the multiple chamber outflows was automatically controlled by a custom-built solenoid multiplexer controlled by LabChart 7 (ADInstruments). At most, three animals were measured at any given time and each chamber was sequentially sampled for 120 s during the course of the run. An additional solenoid allowed for sampling of the inflow O_2 levels between the sampling of the chambers to account for any potential drift. Rates of oxygen consumption ($\dot{V}_{O_2}$; ml O_2 min^{-1}) were calculated using the following equation (Withers, 2001):

$$\dot{V}_{O_2} = \dot{V}_I \times \frac{(F_{I_{O_2}} - F_{E_{O_2}})}{1 - F_{E_{O_2}}} \quad (1)$$

where $\dot{V}_I$ is incurrent flow rate (ml min^{-1}), $F_{I_{O_2}}$ is the incurrent O_2 fraction of dry gas and $F_{E_{O_2}}$ is the excurrent O_2 fraction of dry gas. A subset of the externally pipped and day 0 hatching $\dot{V}_{O_2}$ data was initially reported in Sirsat and Dzialowski (2016).

Following measurement of metabolic rate, animals were euthanized with isoflurane. We then measured masses of whole body, yolk or yolk sac, heart ventricles and liver. Measurements were conducted on embryos on day 24 or 25 of incubation (28-day total incubation period), during internal pipping and external pipping, and on hatchlings on days 0, 3 and 7 post-hatch. In another set of animals, we measured yolk-free body mass, iliotibialis and femorotibialis muscle groups of the right thigh, and pectoralis major muscle of the right breast from day 25 embryos, externally pipped paranates, and hatchlings during the first day of post-hatch life.

Preparation of permeabilized muscle fibers

Mitochondrial respiration was measured in permeabilized skeletal muscle fibers from the femorotibialis muscle of the right thigh and pectoralis major muscle of the right breast, and from both right and left cardiac ventricle wall muscles. Muscle samples were removed from the animal when other body parts were dissected, and were prepared for measurement according to Pesta and Gnaiger (2012). Muscle samples were placed in ice-cold BIOPS solution (in mmol l^{-1}: 2.77 CaK_2EGTA, 7.23 K_2EGTA, 5.77 Na_2ATP, 6.56 $MgCl_2{\times}6H_2O$, 20 taurine, 15 Na_2-phosphocreatine, 20 imidazole, 0.5 dithiothreitol and 50 4-morpholineethanesulfonic acid; pH 7.1) and then carefully teased apart with fine-tipped forceps while in the ice-cold BIOPS. Tissues were then gently shaken for 30 min in 2 ml of BIOPS containing 50 µg ml^{-1} saponin to permeabilize the fibers at 4°C. The tissues were then washed three times for 10 min each in 2 ml of respiration assay medium (in mmol l^{-1}: 0.5 EGTA, 3 $MgCl_2$, 60 lactobionic acid, 20 taurine, 10 KH_2PO_4, 20 HEPES, 110 sucrose and 1 g l^{-1} BSA; pH 7.1) with gentle mixing. Fibers were blotted dry on a Kimwipe, weighed (Analytical XA Balance,

Journal of Experimental Biology (2016) 219, 1214-1223 doi:10.1242/jeb.132282

Mettler-Toledo, Columbus, OH, USA) and placed in a respiration chamber.

Mitochondrial respiration

In situ mitochondrial respiration was measured with an Oxygraph-2k high-resolution respirometer (Oroboros, Innsbruck, Austria) at 38°C (Fig. 1). Permeabilized skeletal muscle fibers weighing between 3 and 5 mg wet mass were placed into 2 ml of respiration assay medium containing catalase (280 units ml^{-1}) in the respiration chamber. A hyperoxygenated environment in the respiration chamber was produced by addition of 2–5 µl H_2O_2 (200 mmol l^{-1}) to avoid any potential limitations in O_2 diffusion into the permeabilized fibers (Pesta and Gnaiger, 2012). Upon stabilization of oxygen consumption, malate (0.5 mmol l^{-1}) and glutamate (10 mmol l^{-1}) were added to stimulate non-phosphorylating 'resting' mitochondrial respiration in the absence of adenylates ($LEAK_N$). This was followed by addition of 5 mmol l^{-1} ADP to stimulate oxidative phosphorylation through complex I ($OXPHOS_{CI}$). Then, 10 µmol l^{-1} cytochrome *c* was provided to test for mitochondrial membrane integrity. Because cytochrome *c* cannot cross an intact outer mitochondrial membrane, an increase in oxygen flux indicates damaged mitochondria. Succinate (20 mmol l^{-1}) was then provided to stimulate oxidative phosphorylation through complexes I and II ($OXPHOS_{CI+CII}$). Finally, multiple injections of 1 µmol l^{-1} carbonylcyanide *p*-trifluoromethoxy-phenylhydrazone (FCCP) were given to stimulate maximal non-coupled complex I+II electron transport system (ETS) capacity. Cardiac muscle and skeletal muscle oxygen flux measurements that exhibited an increased flux of more than 12% after addition of cytochrome *c* were not included in the analysis. In skeletal muscle, we increased the cut-off to 18% for embryonic day 24 and externally pipped samples because of the low flux rates. All chemicals were obtained from Sigma-Aldrich (St Louis, MO, USA).

Statistics

Comparisons of organ and body masses were carried out by one-way ANOVA with age as a factor, followed by a Holm–Sidak *post hoc* test. Tissue masses as a percentage of yolk-free body mass were calculated by dividing the tissue mass by yolk-free body mass. Regressions of heart ventricle mass on yolk-free body mass were performed on log-transformed data. To examine changes in $\dot{V}_{O_2}$ with age, we analyzed resting $\dot{V}_{O_2}$ three ways: as whole-animal $\dot{V}_{O_2}$ using a one-way ANOVA, as mass-specific $\dot{V}_{O_2}$ after dividing $\dot{V}_{O_2}$ by yolk-free body mass using a one-way ANOVA, and as $\dot{V}_{O_2}$ corrected for yolk-free body mass with a one-way ANCOVA with yolk-free body mass as a covariate. For each $\dot{V}_{O_2}$ analysis we used age as the factor followed by a Holm–Sidak *post hoc* test. Mass-specific $\dot{V}_{O_2}$ was log transformed prior to analysis. Changes in whole-animal metabolic rate during cooling were analyzed within each age by determining the thermal neutral zone using a modified method of Yeager and Ultsch (1989) programmed in R. This method was originally developed to find two regressions that minimize the sum of squares to determine cut-off points for the critical partial pressure of O_2. Instead of attempting to minimize the sum of squares of the two regressions, we determined the range of ambient temperatures across which the slope was closest to zero for air temperatures in the thermal neutral zone. To determine changes in permeabilized oxygen flux of each tissue type (breast, thigh, left ventricle, or right ventricle) with development, one-way ANOVAs with age were carried out followed by a Holm–Sidak *post hoc* test against the embryonic day 24 value. Because we were interested in determining whether there were differences between thigh and breast or right and left ventricle on each day, we compared values on each day of development with multiple *t*-tests followed with a Holm–Sidak correction to take into account the multiple tests. The permeabilized muscle fiber data were log transformed prior to analysis, but are presented as raw means. Statistical analyses were conducted using SigmaPlot 12 (Systat Software, San Jose, CA, USA) and Prism 6 (GraphPad Software, La Jolla, CA, USA). Sample sizes are provided in the figures. The level of significance was set at $P<0.05$. All data are presented as means±s.e.m.

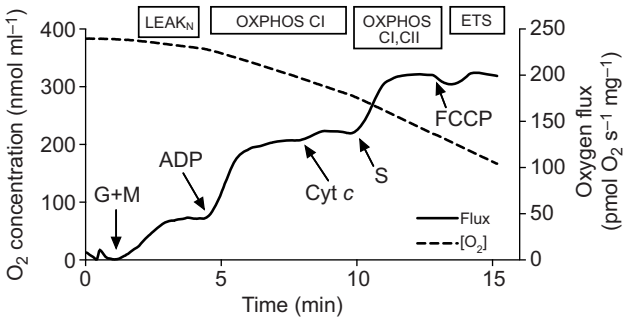

Fig. 1. Representative trace of O_2 concentration and O_2 flux from permeabilized cardiac muscle cells in Pekin duck. G, glutamate (10 mmol l^{-1}); M, malate (2 mmol l^{-1}); ADP (5 mmol l^{-1}); Cyt *c*, cytochrome *c* (10 µmol l^{-1}); S, succinate (10 mmol l^{-1}); FCCP, carbonylcyanide *p*-trifluoromethoxy-phenylhydrazone (1 µmol l^{-1}). Dashed line indicates oxygen concentration and solid line indicates oxygen flux.

RESULTS

Oxygen consumption and thermoregulatory capacity

Though statistical significance of developmental changes in resting $\dot{V}_{O_2}$ depended upon the way in which $\dot{V}_{O_2}$ was presented, a noteworthy change in metabolism occurred concomitantly with hatching. Whole-animal $\dot{V}_{O_2}$ in the thermal neutral zone increased significantly with development ($F_{4,27}=72.0$, $P<0.0001$; Table 1). Mass-specific $\dot{V}_{O_2}$ did not increase until after hatching ($F_{4,23}=24.4$, $P<0.001$; Table 1). When $\dot{V}_{O_2}$ was analyzed by ANCOVA, the yolk-free body mass covariate was not significant ($F_{1,22}=1.7$, $P=0.205$), but age was significant ($F_{4,22}=13.4$, $P<0.001$). When $\dot{V}_{O_2}$ was evaluated at a yolk-free body mass of 54.2 g, day 3 hatchlings had metabolic rates that were higher than those at the other ages (Table 1).

Endothermic capacity, manifested as an increase in $\dot{V}_{O_2}$ as air temperature (T_a) decreased, did not appear until after hatching in Pekin ducks (Fig. 2). On day 24 of incubation and during the initial paranatal phase of internal pipping, $\dot{V}_{O_2}$ initially remained constant with the onset of cooling. Then, at both ages, $\dot{V}_{O_2}$ began to decrease as air temperature reached 30°C and steadily decreased with cooling. The mean response of externally pipped paranates was maintenance of a constant $\dot{V}_{O_2}$ as air temperature decreased from 37°C to 20°C.

Upon hatching, $\dot{V}_{O_2}$ exhibited an endothermic response with a clear thermal neutral zone followed by a linear increase in $\dot{V}_{O_2}$ with further cooling below the lower critical temperature (Fig. 2). The lower critical temperature of day 0 hatchlings was 32.2°C and the thermal neutral zone extended to 25.4°C in day 3 hatchlings. All hatchlings were able to maintain an elevated $\dot{V}_{O_2}$ down to the lowest T_a tested, 15°C.

Mass

Yolk-free body mass ($F_{5,141}=160.1$, $P<0.001$; Fig. 3A), cardiac ventricle mass ($F_{5,139}=99.0$, $P<0.001$; Fig. 3B) and liver mass

Journal of Experimental Biology (2016) 219, 1214-1223 doi:10.1242/jeb.132282

Table 1. Whole-animal $\dot{V}_{O_2}$, mass-specific $\dot{V}_{O_2}$ and mass-corrected $\dot{V}_{O_2}$ (at a yolk-free body mass of 54.2 g) for embryos at an air temperature of 35°C and hatchlings within their thermal neutral zone

Stage	Whole-animal $\dot{V}_{O_2}$ (ml O_2 min^{-1})	Mass-specific $\dot{V}_{O_2}$ (ml O_2 h^{-1} g^{-1})	Mass-corrected $\dot{V}_{O_2}$ (ml O_2 min^{-1})
E24	0.42±0.07[a]	0.75±0.06[a]	0.72±0.27[a,b]
IP	0.67±0.04[a,b]	0.87±0.12[a]	0.77±0.15[a]
EP	0.97±0.09[b,c]	1.06±0.09[a]	0.96±0.72[a,b]
D0	1.27±0.04[c]	1.50±0.06[b]	1.32±0.12[b]
D3	2.47±0.13[d]	2.14±0.14[c]	2.25±0.19[c]

Whole-animal and mass-specific $\dot{V}_{O_2}$ were analyzed using one-way ANOVA, and mass-corrected $\dot{V}_{O_2}$ using one-way ANCOVA with yolk-free body mass as a covariate. ANOVAs for mass-specific $\dot{V}_{O_2}$ were carried out after log transformation. Data with different letters are significantly different at $P<0.05$. E24, day 24 embryos; IP, internally pipped paranates; EP, externally pipped paranates; D0, day 0 post-hatching; D3, day 3 post-hatching.

($F_{5,125}$=136.8, P<0.001; Fig. 3C) increased significantly with age. From day 24 of incubation to the internally pipped stage, yolk-free body mass increased significantly (P=0.002). This increase was followed by a plateau in body mass from the internally pipped stage through the first day of post-hatch life in which there were no significant changes in yolk-free body mass. Between days 0 and 7 post-hatching, yolk-free body mass increased significantly.

Cardiac ventricle mass followed a developmental pattern with an inflection at hatching. There was a gradual increase in ventricle mass from embryonic day 24 through external pipping (Fig. 3B). Ventricle mass then increased significantly between external pipping and the first day of post-hatch life (P<0.001). This increase in cardiac ventricle mass occurred without a similar increase in yolk-free body mass (Fig. 4). In the neonatal stage, cardiac ventricle mass continued to increase with an increase in yolk-free body mass (Fig. 4). Thus, cardiac ventricle mass had two distinct scalings with body mass, with a transition occurring between external pipping and hatching. Because body mass remained relatively constant from internal pipping through the first day of post-hatch life, the fraction of the body that was cardiac ventricle increased significantly ($F_{5,137}$=31.4, P<0.001; Fig. 3B), almost doubling between internal pipping and day 0 post-hatching.

Liver mass and the percent of the body composed of liver did not increase significantly until days 0 and 3 post-hatch (Fig. 3C).

Masses of pectoralis (breast) and iliotibialis and femorotibialis (thigh group) skeletal muscles differed with age (Fig. 5). From the day 25 embryo through the first day of post-hatch life, there was a significant increase in both absolute mass ($F_{2,34}$=30.3, P<0.001) and percentage of the animal composed of the right thigh skeletal muscle ($F_{2,34}$=19.4, P<0.001; Fig. 5B). This occurred without any change in yolk-free body mass from the externally pipped paranate to the first day of post-hatch life (Fig. 5A). In contrast, there was a significant decrease in absolute mass of the right breast muscle in the day 0 hatchling ($F_{2,34}$=3.9, P=0.03; Fig. 5C). The percentage of the animal composed of the right breast muscle decreased significantly with age ($F_{2,34}$=76.3, P<0.001).

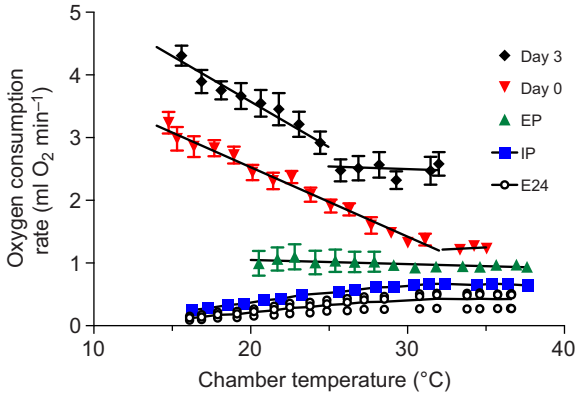

Fig. 2. Whole-animal oxygen consumption in response to cooling. Oxygen consumption rate (ml O_2 min^{-1}) of Pekin ducks at late embryonic stage day 24 (E24, n=3), internally pipped (IP, n=7) and externally pipped (EP, n=9) paranates, and hatchlings on day 0 (D0, n=6) and day 3 (D3, n=7) post-hatching in response to cooling at a rate of 9.2°C h^{-1}. Data are presented as means±s.e.m.

Mitochondria respiration in permeabilized fibers

Both muscle type (thigh and breast) and ontogeny affected mitochondrial oxygen flux capacity in skeletal muscle (Fig. 6). $LEAK_N$ increased significantly with age in the thigh muscle ($F_{4,44}$=12.56, P<0.001), but not breast ($F_{4,35}$=1.04, P=0.4). Thigh muscle $LEAK_N$ was significantly higher in hatchlings than in day 24 embryos (Fig. 6A). Differences between thigh and breast also occurred in $OXPHOS_{CI}$ and $OXPHOS_{CI+CII}$ capacities, with thigh fibers having a significantly higher flux capacity than breast fibers at all ages (all corrected P<0.003; Fig. 6B,C). Developmentally, there was a significant increase in $OXPHOS_{CI}$ flux in both thigh ($F_{4,44}$=13.2, P<0.001) and breast fibers ($F_{4,35}$=5.6, P=0.001) upon hatching. $OXPHOS_{CI+CII}$ flux capacity of thigh ($F_{4,44}$=9.3, P<0.001) and breast fibers ($F_{4,35}$=6.2, P<0.001) increased significantly from external pipping through hatching. $LEAK_N$ versus $OXPHOS_{CI}$ and $OXPHOS_{CI}$ versus $OXPHOS_{CI+CII}$ did not differ between ages or tissues (Fig. 6D,E). The flux control ratio of $OXPHOS_{CI+CII}$ to ETS was close to 1 for all ages and both tissues, suggesting there is little reserve capacity in the phosphorylating system as there was no increase in non-coupled ETS respiratory flux upon addition of FCCP (Fig. 6F).

Right and left cardiac ventricle mitochondrial $OXPHOS_{CI}$ and $OXPHOS_{CI+CII}$ capacity increased significantly with development (Fig. 7). $LEAK_N$ capacity of right ventricle ($F_{5,32}$=1.52, P=0.21) and left ventricle ($F_{5,38}$=2.05, P=0.093) did not change during development or differ between right and left sides (Fig. 7A). $OXPHOS_{CI}$ capacity increased significantly in both right ($F_{5,32}$=5.72, P<0.001) and left ventricle ($F_{5,38}$=8.55, P<0.001) upon hatching (Fig. 7B) and although $OXPHOS_{CI+CII}$ capacity increased in both right and left ventricle with hatching, the increase was only significant in the left ventricle ($F_{5,38}$=5.53, P<0.001; Fig. 7C). There were no differences in the ratio of $LEAK_N$ versus $OXPHOS_{CI}$ between sides or among ages (Fig. 7D). Addition of succinate resulted in an increase in $OXPHOS_{CI+CII}$ capacity over $OXPHOS_{CI}$ capacity at all ages and in both sides of the ventricle, as can be observed by the $OXPHOS_{CI}/OXPHOS_{CI+CII}$ ratio being less than 1 (Fig. 7E). On days 3 and 7 post-hatch, left ventricle $OXPHOS_{CI+CII}$ flux capacity increased significantly compared with day 24 embryos (Fig. 7C). As with skeletal muscle, no increase in oxygen flux with the addition of FCCP was observed, such that the $OXPHOS_{CI+CII}$ to ETS flux control ratio was close to 1 (Fig. 7F). The $OXPHOS_{CI}$ and $OXPHOS_{CI+CII}$ flux capacities of the left

Journal of Experimental Biology (2016) 219, 1214-1223 doi:10.1242/jeb.132282

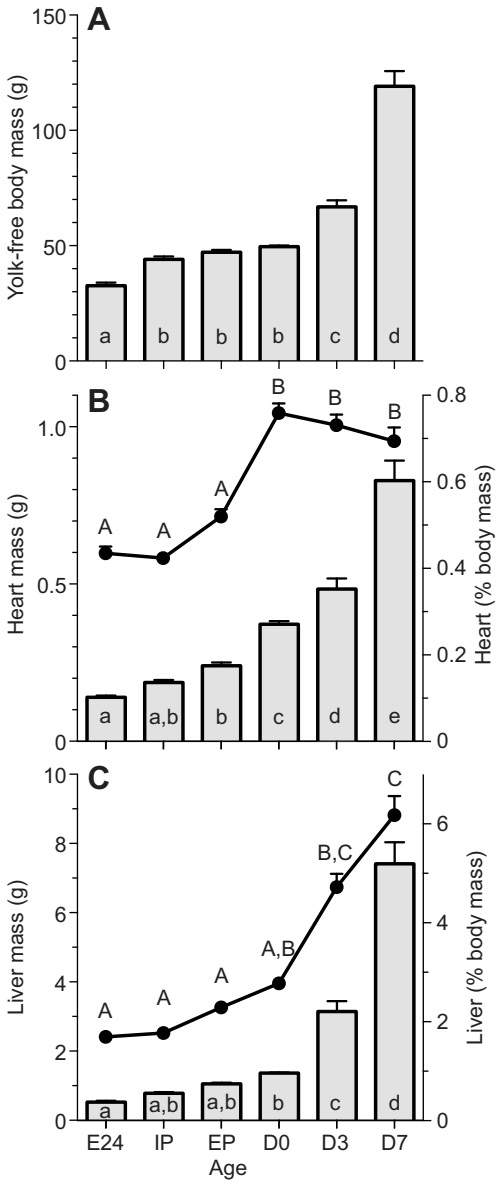

Fig. 3. Morphological traits of Pekin ducks from the late embryonic stages through day 7 post-hatching. (A) Yolk-free body mass (g), (B) heart mass (g) and percentage of the body composed of the heart, and (C) liver mass (g) and percentage of the body composed of the liver for day 24 embryos (E24; *n*=17, 17, 9), internally pipped (IP; *n*=18, 18, 18) and externally pipped (EP; *n*=16, 18, 17) paranates, and hatchlings on day 0 (D0; *n*=63, 63, 57), day 3 (D3; *n*=19, 15, 16) and day 7 (D7; *n*=14, 14, 14) post-hatching. In B and C, organ mass is presented as bars and the percent of the body composed of the organ is shown by the line. Data with different letters are significantly different at $P<0.05$ (Holm–Sidak *post hoc* test). Data are presented as means±s.e.m.

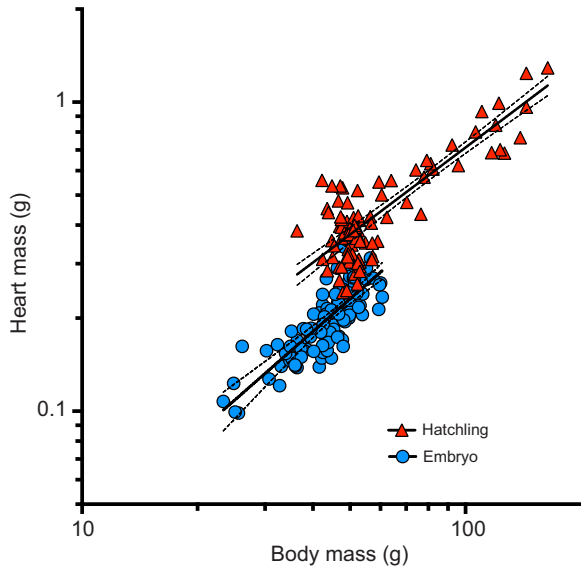

Fig. 4. Relationship between heart mass (M_h, g) and yolk-free embryo mass (M_e, g) in Pekin duck. Data are from embryos from day 24 of incubation through external pipping (circles; *n*=108, $M_h=-2.45M_e^{1.09}$, $r^2=0.56$) and hatchlings 0 to 7 days post-hatch (triangles; *n*=92, $M_h=-2.02M_e^{0.94}$, $r^2=0.79$). Dashed lines represent 95% confidence limits for the linear regression mean.

ventricle were higher in the oldest hatchlings compared with $OXPHOS_{CI}$ and $OXPHOS_{CI+CII}$ flux capacities of the right ventricle, but these differences were not significant (Fig. 7B,C).

DISCUSSION

An endothermic phenotype requires an elevated capacity to deliver oxygen from the environment to mitochondria and elevated skeletal muscle mitochondria OXPHOS capacity for shivering and non-shivering thermogenesis. Similar to other precocial species, Pekin ducks rapidly attained an endothermic phenotype after hatching and, consequently, an increased cellular energy demand associated with heat generation during periods of cold thermal stress. We found that attainment of endothermy at hatching in Pekin duck was marked by increased heart mass, thigh skeletal muscle mass and mitochondrial OXPHOS capacity in skeletal and cardiac muscle. These augmentations, along with an increase in ventilation (Sirsat and Dzialowski, 2016), appear to work in concert to meet the increased energy demands of the endothermic phenotype that is maturing during transition to the neonatal period and are in contrast to the lack of change in hatching and neonatal ectotherms (Sirsat et al., 2016).

Development of metabolic endothermic response

The Pekin duck is a precocial species that develops an endothermic phenotype rapidly upon hatching (Fig. 2). During embryonic and internal pipping stages, the embryos exhibit an ectothermic phenotype. $\dot{V}_{O_2}$ was maintained during the initial cooling of the egg/embryo, but began to decrease when ambient temperature reached 30°C for both day 24 embryos and internally pipped embryos. During external pipping, the $\dot{V}_{O_2}$ response was intermediate between that of an ectotherm and endotherm. Although, individually, $\dot{V}_{O_2}$ decreased, remained constant or increased in different externally pipped animals, the mean response of all externally pipped embryos was to maintain $\dot{V}_{O_2}$ across all temperatures tested. The different responses may have been due to differences in length of time an animal was in the external pipping stage; longer periods at the external pipping stage may have allowed for more development of metabolic pathways and increased lung ventilation (Sirsat and Dzialowski, 2016). At this stage, both the respiratory and cardiovascular systems may limit oxygen delivery. Given the lower OXPHOS capacity of both the skeletal muscle and the heart (Figs 6, 7), these animals were probably also limited in their capacity to generate heat by both shivering and non-shivering thermogenesis.

Upon hatching, the Pekin duck was able to increase $\dot{V}_{O_2}$ and concomitant heat production, allowing hatchlings to exhibit an

Journal of Experimental Biology

Journal of Experimental Biology (2016) 219, 1214-1223 doi:10.1242/jeb.132282

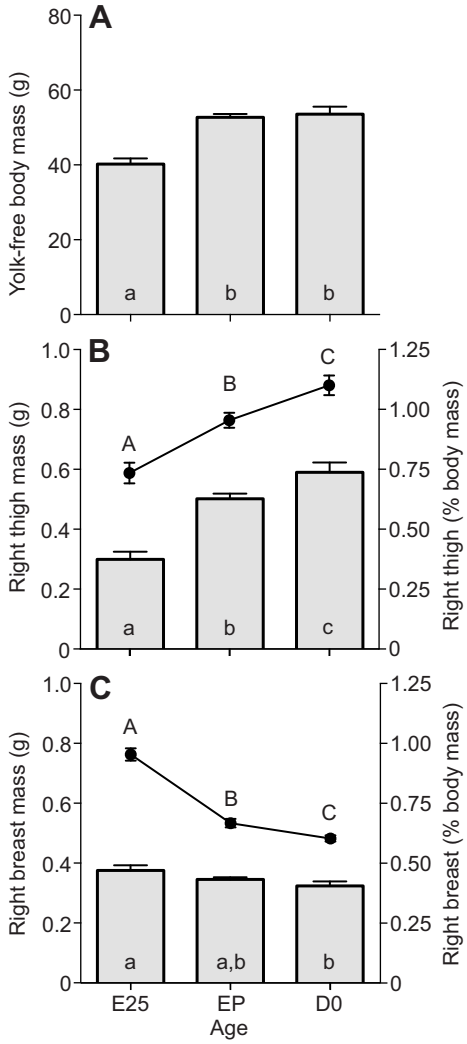

Fig. 5. Developmental trajectory of thigh and breast skeletal muscle from late embryonic stage through day 0 post-hatching in Pekin duck. (A) Yolk-free body mass (g), (B) right thigh skeletal muscle (g) and percentage of the body composed of the right thigh muscle (%), and (C) right breast muscle (g) and percentage of the body composed of the right breast muscle (%) for day 25 embryos (E25; *n*=9), externally pipped paranates (EP; *n*=17) and hatchlings within the first 24 h of hatching (D0; *n*=11). Data with different letters are significantly different at $P<0.05$ (ANOVA followed by Holm–Sidak *post hoc* test). Data are presented as means±s.e.m.

endothermic phenotype. All day 0 hatchlings showed the typical endothermic response, with a thermal neutral zone and increasing $\dot{V}_{O_2}$ occurring below a lower critical temperature (Fig. 2). Other precocial bird species have shown similar rapid attainment of an endothermic phenotype upon hatching (Steen and Gabrielsen, 1986; Dzialowski et al., 2007). The endothermic response does not appear to be limited by the capacity of any one step in the oxygen cascade after the ducks hatch, as predicted by Whittow and Tazawa (1991). From day 0 to day 3 of post-hatch life there is an increase in the thermal neutral zone. This may reflect an increase in insulation with age or changes in the surface area to volume ratio.

Morphological changes associated with endothermy

During the paranatal stage, from internal pipping to hatching and when the metamorphosis from ectothermy to endothermy occurs, there was very little change in yolk-free body mass (Fig. 3A) coincident with noteworthy growth of the heart (Figs 3B and 4). We found that heart mass, a surrogate for stroke volume and capacity for convective O_2 movement by the circulatory system, almost doubled in a span of 24 h, while the ducks transitioned from the externally pipped to the hatchling stage and became endothermic. The cardiac ventricle of the white leghorn chicken and emu significantly increase in mass, with no change in yolk-free body mass, during this same transition from external pipping to hatching (Killpack, 2005; Shell et al., 2016). During embryonic development, relative ventricle mass to yolk-free body mass of the duck is similar to that found in embryonic and juvenile ectotherms (Sirsat et al., 2016). Thus, the cardiovascular system, which may be the limiting step in the O_2 cascade controlling maximal aerobic metabolism (Hillman et al., 2013), seems to be upregulated at hatching to support increased aerobic metabolic capacity associated with endothermy.

The rapid increase in heart mass, associated with the onset of endothermy, is akin to changes seen in infrequent feeders such as pythons during feeding (Riquelme et al., 2011). In the feeding python, the increase in cardiac ventricle mass is due to hypertrophy and not hyperplasia. Snelling et al. (2015b) found that heart mass of grey kangaroo joeys grows hyperallometrically while the joeys are in the pouch, as they approach attaining endothermy and leaving the pouch. Associated changes at the cellular level in the heart also occur within the joey, with increases in mitochondria volume and muscle contractile machinery associated with leaving the pouch and obtaining endothermy (Snelling et al., 2015a). Through day 42 post-hatching in the chicken, ventricle size increases through both hyperplasia and hypertrophy after hatching (Li et al., 1997). It remains to be seen in the Pekin duck whether the increase in ventricle mass associated with the transition to endothermy is due to hypertrophic or hyperplasic growth of the hatchling heart.

Growth of the heart did not occur in anticipation of hatching, but concomitant with hatching and attaining endothermy. During hatching, there is a change in circulation as the atrial foramen and the ductus arteriosus close (Dzialowski et al., 2011). With this change, the animal goes from having pulmonary and systemic circulations in parallel, like most other reptiles, to having them in series and with a separation of pulmonary and systemic pressures. Between embryonic day 20 and the first day of post-hatch life, mean systemic arterial pressure of the chicken doubles from 24.5 to 48.7 mmHg (Girard, 1973). Mean systemic arterial pressure also increases during birth in the lamb (Bartelds et al., 2000). Similar changes in arterial pressure likely occur in the hatching duck. The increase in heart mass may in part be to help the left ventricle produce greater systemic pressures and cardiac outputs associated with an endothermic phenotype. However, it remains to be seen whether the increase in ventricle mass occurs in the left ventricle, right ventricle or both ventricles.

Liver mass and fractional liver mass increased monotonically with age (Fig. 3C). The metabolically active organs of endotherms are typically larger than the same organs in ectotherms (Hulbert and Else, 1989). During the egg stage, the liver of the duck makes up a similar fraction of body mass as found in the embryonic alligator and snapping turtle (Sirsat et al., 2016). After hatching, the duck liver increases in proportion to body mass, while that of ectothermic species remains relatively constant. In European shag nestlings, resting $\dot{V}_{O_2}$ was significantly correlated with liver mass (Moe et al., 2004). The increase in liver mass from the internal pipping stage to 0 days post-hatch may play a role in increasing basal or resting $\dot{V}_{O_2}$ of the hatchling.

Journal of Experimental Biology (2016) 219, 1214-1223 doi:10.1242/jeb.132282

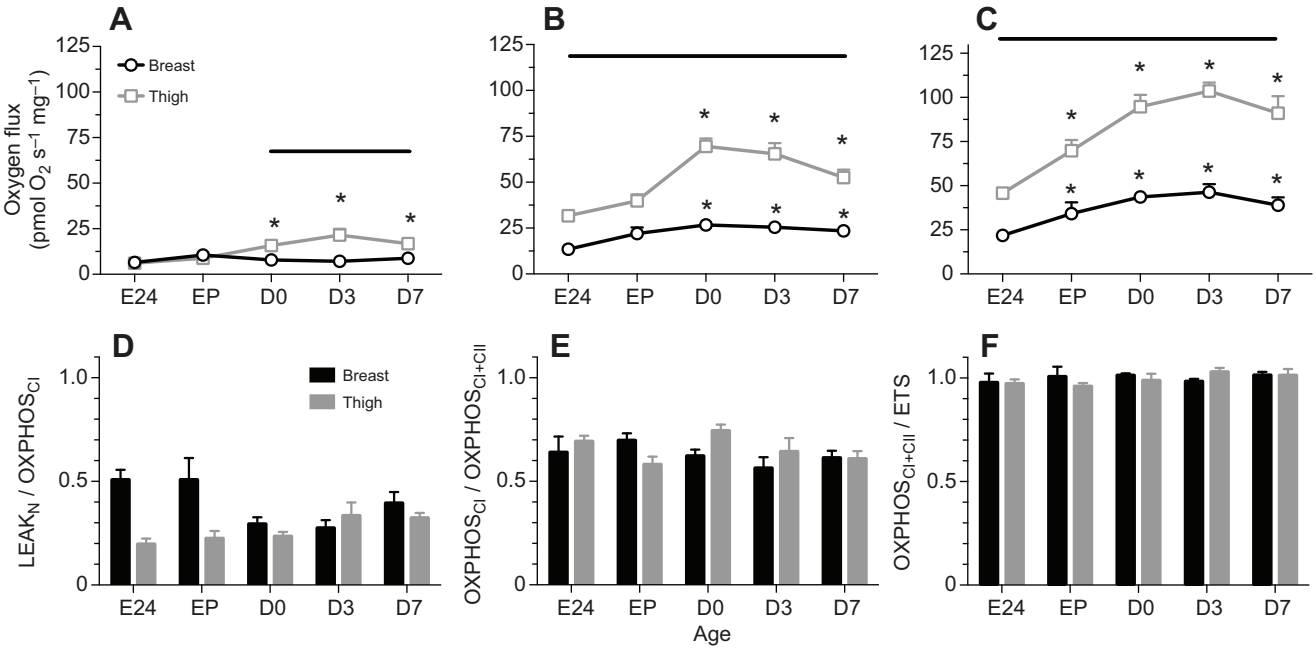

Fig. 6. Developmental changes in mitochondria oxygen flux from permeabilized Pekin duck thigh and breast skeletal muscle. (A) Non-phosphorylating $LEAK_N$ respiration with glutamate and malate as substrates. (B) OXPHOS through complex I in the presence of ADP. (C) OXPHOS through complexes I and II after addition of succinate. (D) Complex I-linked $LEAK_N$ control ratios, calculated as the CI-linked LEAK respiration in the absence of adenylates divided by the uninhibited $OXPHOS_{CI}$ flux. (E) Complex I-linked OXPHOS flux control ratio CI/(CI+II). (F) Phosphorylation system coupling control ratio. Breast sample sizes are: E24 n=7, EP n=5, day 0 n=8, day 3 n=7, and day 7 n=13; thigh sample sizes are: E24 n=6, EP n=10, day 0 n=10, day 3 n=8, and day 7 n=15. Asterisks indicate values that are significantly different from those of stage 24 embryos at P<0.05 for thigh and breast (one-way ANOVA for each tissue, followed by Holm–Sidak *post hoc* test). Horizontal line above the data indicates significant differences between thigh and breast oxygen flux at a given age (*t*-tests followed by Holm–Sidak correction for multiple tests). Data are presented as means±s.e.m.

Maturation of mitochondria function

Skeletal muscle

The OXPHOS capacity of skeletal muscle increased after hatching concomitant with hatchlings attaining an endothermic phenotype. Skeletal muscles are the major source of heat production in birds, through shivering thermogenesis (Marjoniemi and Hohtola, 1999; Hohtola, 2004) or potentially non-shivering thermogenesis (Duchamp and Barre, 1993). As such, there should be an increase in OXPHOS capacity in those muscles associated with enhanced heat production and attainment of an endothermic phenotype. All measures of oxygen flux of the duck permeabilized skeletal muscle fibers were greater in the thigh compared with the breast (Fig. 6). This occurred in association with an increase in thigh muscle mass, while breast muscle mass did not change (Fig. 5). The greater increase in OXPHOS capacity and muscle mass (Fig. 5B) in thigh muscle is associated with these muscles serving as the major site of shivering thermogenesis and contribution to locomotor activity after hatching, a pattern observed in other precocial species; for example, not until the second week post-hatching did Japanese quail, grey partridge and domestic fowl began to use their breast muscle for shivering thermogenesis (Marjoniemi and Hohtola, 1999). Bobwhite (*Colinus virginianus*) and Japanese quail (*Coturnix coturnix japonica*) initially use leg muscles for shivering heat production and develop aerobic capacity as measured by increased citrate synthase activity rapidly upon hatching (Choi et al., 1993).

There was a significant increase in the $LEAK_N$ respiration with increasing age in thigh muscle of Pekin ducks, with little change in breast muscle (Fig. 6). $LEAK_N$ provides a measure of uncoupling due to proton leak and slip across the mitochondrial membrane (Pesta and Gnaiger, 2012). Endotherms typically have leakier membranes than do ectotherms (Hulbert and Else, 1989; Brand et al., 1991). Therefore, one might expect differences in $LEAK_N$ in tissues during the embryonic ectothermic stage compared with the hatchling that has attained endothermy. An increase in $LEAK_N$ was observed in thigh, but not breast, with maturation of endothermic phenotype. Walter and Seebacher (2009) demonstrated an age-related increase in oligomycin-stimulated leak of isolated skeletal muscle mitochondria in the chicken after hatching. They proposed that increased leak might be due to increased ANT-induced uncoupling with development from the embryo to 8 days post-hatching. Hatchling Pekin duck $LEAK_N$ respiration is also higher than that measured in thigh muscles of snapping turtle hatchlings and alligator hatchlings and yearlings (Sirsat et al., 2016).

OXPHOS capacity of mitochondria in thigh and breast skeletal muscle increased between external pipping and the first day of hatching in Pekin ducks (Fig. 6). During ectothermic embryo stages, levels of both $OXPHOS_{CI}$ and $OXPHOS_{CI+CII}$ oxygen flux in the duck breast were similar to those of hatchling alligator and snapping turtles (Sirsat et al., 2016). The significant increase in OXPHOS capacity of thigh muscle was coincident with attainment of endothermic phenotype and increased locomotor activity on the first day of post-hatch life. This increase in thigh and breast OXPHOS capacity upon hatching was not observed in either alligator or snapping turtle hatchlings (Sirsat et al., 2016). During the external pipping stage, the embryo exhibited an intermediate $\dot{V}_{O_2}$ response to cooling, which may in part be limited by the OXPHOS capacity of skeletal muscles.

Very few studies have examined developmental trajectories of *in situ* mitochondrial function in permeabilized fibers in avian or mammalian skeletal muscle. Permeabilized pectoralis muscle fiber $OXPHOS_{CI+CII}$ capacity in semi-altricial Adélie penguin chicks did not change from day 7 to day 15 of post-hatch life, even though at

Journal of Experimental Biology (2016) 219, 1214-1223 doi:10.1242/jeb.132282

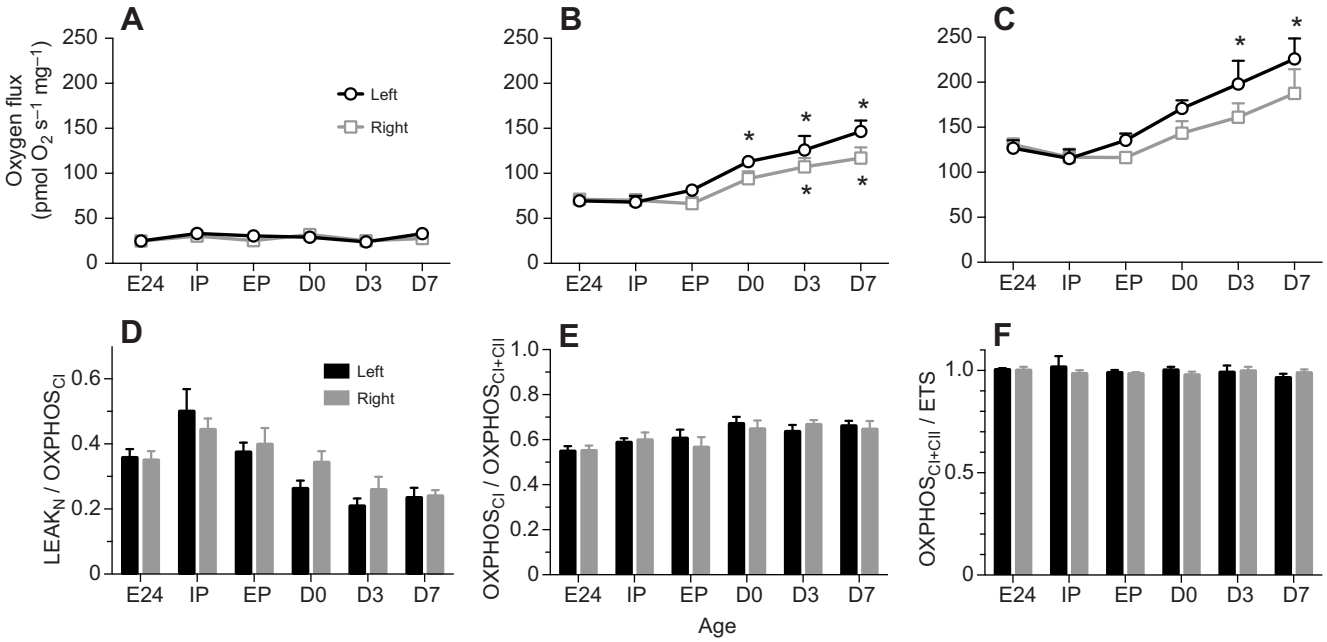

Fig. 7. Developmental changes in mitochondria oxygen flux from permeabilized duck right and left cardiac ventricle. (A) Non-phosphorylating $LEAK_N$ respiration with glutamate and malate as substrates. (B) OXPHOS through complex I in the presence of ADP. (C) OXPHOS through complexes I and II after addition of succinate. (D) Complex I-linked $LEAK_N$ control ratios, calculated as the CI-linked LEAK respiration in the absence of adenylates divided by the uninhibited $OXPHOS_{CI}$ flux. (E) Complex I-linked OXPHOS flux control ratio CI/(CI+II). (F) Phosphorylation system coupling control ratio. Left cardiac ventricle samples sizes are: E24 *n*=6, IP *n*=5, EP *n*=5, day 0 *n*=11, day 3 *n*=9, and day 7 *n*=8; right cardiac ventricle sample sizes are: E24 *n*=6, IP *n*=5, EP *n*=6, day 0 *n*=6, day 3 *n*=9, and day 7 *n*=6. Asterisks indicate values that are significantly different from those of stage 24 embryos at $P<0.05$ for left and right ventricles (one-way ANOVA for each tissue, followed by Holm–Sidak *post hoc* test). Data are presented as means±s.e.m.

day 15 the animals were beginning to be endothermic (Fongy et al., 2013). $OXPHOS_{CI+CII}$ capacity in penguin chicks was significantly lower than that of adults and those measured in our study animals. Our measured levels of $OXPHOS_{CI+CII}$ capacity in the duck thigh muscle were similar to levels measured in human vastus lateralis muscles (Chicco et al., 2014). Other studies examining metabolic enzyme development in skeletal muscles have revealed similar developmental trends as those shown here (e.g. Choi et al., 1993). Eider ducks showed a rapid increase in cytochrome *c* oxidase activity in thigh muscle during the first day of post-hatch life, and levels remained elevated through at least the first 2 days of post-hatch life (Grav et al., 1988).

Though not measured in our study, the increase in OXPHOS capacity of the thigh skeletal muscle that coincides with attainment of endothermy is probably due to an increase in mitochondria number in the cells. There is over a twofold increase in permeabilized fiber OXPHOS capacity from embryonic stage 24 to the third day post-hatch. During hatching, the mitochondria density in *iliofibularis* leg muscle of the chicken increased 3.8-fold from just prior to internal pipping to post-hatch day 4 (Eppley and Russell, 1995). Mitochondrial density in skeletal muscle differs between endothermic and ectothermic species (Else and Hulbert, 1985). Thus, the changes seen in OXPHOS capacity between the two stages in the duck are likely due to increased mitochondria numbers.

Cardiac muscle

The OXPHOS capacity of the right and left ventricles increased significantly, concomitant with the increase in ventricle mass and attainment of endothermy. This increase in OXPHOS capacity begins to occur after hatching, during a time in development when the animal becomes endothermic. Maturation of the cardiovascular system and the associated increase in convective O_2 transport are necessary for attaining an endothermic phenotype (Hillman and Hedrick, 2015). Associated with endothermy is an increase in both resting and active cardiac output and cardiac work, due to increased heart rate and stroke work (Hillman and Hedrick, 2015). The adult endothermic heart has one of the highest aerobic basal metabolic rates and must have the capacity to increase work by fourfold to sixfold during aerobic exercise or thermal stress (Lopaschuk et al., 2010). We found that OXPHOS capacity of cardiac myocytes was higher than OXPHOS capacity of skeletal muscle. Few studies have examined both cardiac and skeletal muscle OXPHOS capacity in avian species. OXPHOS capacity was higher in cardiac muscle compared with skeletal muscle in alligator and snapping turtle neonates (Sirsat et al., 2016). In contrast, Zhang et al. (2015) found that citrate synthase activity was higher in breast muscle compared with cardiac muscle in a number of adult passerines.

As noted above, the heart increased in mass significantly between external pipping and the first day of post-hatch life, with little change in yolk-free body mass. This disproportionate increase in mass was accompanied by an increase in OXPHOS capacity of the cardiomyocytes. At this point in development, hatchlings are switching their mode of gas exchange, the ductus arteriosus is closing, and pressures in the systemic circuit should be increasing. These changes would likely require greater work from the ventricles, which would necessitate a greater OXPHOS capacity. Increases in cardiomyocyte OXPHOS capacity after birth have been observed in neonatal rats (Anmann et al., 2014). In contrast, there is little change in OXPHOS capacity of the ectothermic alligator and snapping turtle cardiomyocytes upon hatching, as expected in species that do not transition to an endothermic phenotype (Sirsat et al., 2016).

We anticipate a shift in metabolic substrates associated with hatching and a transition to endothermy of the heart. In mammals at

birth, there is a transition from glucose to fatty acids as a major source of cardiomyocyte fuel (Lopaschuk and Jaswal, 2010). Given the similarities in changes in arterial O_2 levels during hatching and birth between mammals and birds (Tazawa et al., 1983; Berger et al., 1990), one would expect the avian heart to make a similar fuel switch at hatching. OXPHOS by fatty acid metabolism is linked by electron transfer flavoprotein and complex I as major acceptors for the reducing equivalents, with NAD^+/NADH ratios playing a role in controlling β-oxidation. Therefore, one might expect to see an increase in OXPHOS capacity through $OXPHOS_{CI}$ with hatching relative to $OXPHOS_{CI+CII}$. At hatching, there was a slight increase in the flux control ratio of $OXPHOS_{CI}/OXPHOS_{CI+CII}$ of both the right and left ventricle (Fig. 6E). This increase in $OXPHOS_{CI}$ as a greater component of total OXPHOS through complexes I and II at hatching may correspond with a shift from reliance on glucose to fatty acids as substrates.

Perspective and significance

Phenotypes of endothermic animals are distinguished from those of ectotherms by four major characteristics – high basal metabolic rate, high aerobic metabolic capacity and heat production that increase in response to cold thermal stress, and effective insulation that retains internally produced heat. Development of an endothermic phenotype from an ectothermic starting point requires changes in all four characteristics. The precocial Pekin duck hatches at a relatively mature stage with downy insulation and advanced locomotor capability, and has a rapidly developing aerobic capacity and thermogenic capability. In the embryonic stages, mitochondrial capacities of the duck are similar to those of embryonic ectotherms (Sirsat et al., 2016). In the externally pipped stage, Pekin ducks, and probably other highly precocial species, can maintain but cannot increase oxygen consumption and heat production because of limits imposed at multiple levels of the oxygen cascade. Upon hatching, there is a significant increase in both heart ventricle mass and maximal OXPHOS capacity of the heart and skeletal muscle, specifically the thigh muscle, that is not observed in ectothermic species after they hatch (Sirsat et al., 2016). At this point, the thigh is the major site of shivering (and potentially non-shivering) thermogenesis and increased muscle mass, and OXPHOS capacity provides increased capacity for heat generation. Because of increases in capacity to deliver oxygen to the tissues by the cardiovascular and respiratory systems (Sirsat and Dzialowski, 2016) and increased capacity of muscles to utilize oxygen to produce ATP, the Pekin duck completes a 1-day metamorphosis from life as an ectotherm to that of an endotherm. It appears that all four characteristics mature in concert to produce an endothermic metabolic phenotype, with each characteristic contributing a limiting factor.

Acknowledgements

Kimberley Prince helped with collection of permeabilized fiber oxygen flux data.

Competing interests

The authors declare no competing or financial interests.

Author contributions

Designed experiments: S.K.G.S., T.S.S., A.F., P.R.S. and E.M.D. Conducted experiments: S.K.G.S., T.S.S., A.D., S.W., A.F. and E.M.D. Analyzed and interpreted data: S.K.G.S., T.S.S., A.F., S.W., A.D., P.R.S. and E.M.D. Wrote the manuscript: E.M.D. Edited the manuscript: S.K.G.S., T.S.S., A.D., S.W., A.F., P.R.S. and E.M.D.

Funding

This work was supported by the National Science Foundation (IOS 1146758 to E.M.D.).

References

Anmann, T., Varikmaa, M., Timohhina, N., Tepp, K., Shevchuk, I., Chekulayev, V., Saks, V. and Kaambre, T. (2014). Formation of highly organized intracellular structure and energy metabolism in cardiac muscle cells during postnatal development of rat heart. *Biochim. Biophys. Acta.* **1837**, 1350-1361.

Bartelds, B., Knoester, H., Smid, G. B., Takens, J., Visser, G. H., Penninga, L., van der Leij, F. R., Beaufort-Krol, G. C. M., Zijlstra, W. G., Heymans, H. S. A. et al. (2000). Perinatal changes in myocardial metabolism in lambs. *Circulation* **102**, 926-931.

Berger, P. J., Horne, R. S. C., Soust, M., Walker, A. M. and Maloney, J. E. (1990). Breathing at birth and the associated blood gas and pH changes in the lamb. *Respir. Physiol.* **82**, 251-266.

Brand, M. D., Couture, P., Else, P. L., Withers, K. W. and Hulbert, A. J. (1991). Evolution of energy metabolism. Proton permeability of the inner membrane of liver mitochondria is greater in a mammal than in a reptile. *Biochem. J.* **275**, 81-86.

Chicco, A. J., Le, C. H., Schlater, A., Nguyen, A., Kaye, S., Beals, J. W., Scalzo, R. L., Bell, C., Gnaiger, E., Costa, D. P. et al. (2014). High fatty acid oxidation capacity and phosphorylation control despite elevated leak and reduced respiratory capacity in northern elephant seal muscle mitochondria. *J. Exp. Biol.* **217**, 2947-2955.

Choi, I.-H., Ricklefs, R. E. and Shea, R. E. (1993). Skeletal muscle growth, enzyme activities, and the development of thermogenesis: a comparison between altricial and precocial birds. *Physiol. Zool.* **66**, 455-473.

Driedzic, W. R., Sidell, B. D., Stove, D. and Bransombe, R. (1987). Matching of vertebrate cardiac energy demand to energy metabolism. *Am. J. Physiol. Regul. Integr. Comp. Physiol.* **252**, R930-R937.

Duchamp, C. and Barre, H. (1993). Skeletal muscle as the major site of nonshivering thermogenesis in cold-acclimated ducklings. *Am. J. Physiol. Regul. Integr. Comp. Physiol.* **265**, R1076-R1083.

Dzialowski, E. M., Burggren, W. W., Komoro, T. and Tazawa, H. (2007). Development of endothermic metabolic response in embryos and hatchlings of the emu (*Dromaius novaehollandiae*). *Respir. Physiol. Neurobiol.* **155**, 286-292.

Dzialowski, E. M., Sirsat, T., van der Sterren, S. and Villamor, E. (2011). Prenatal cardiovascular shunts in amniotic vertebrates. *Respir. Physiol. Neurobiol.* **178**, 66-74.

Else, P. L. and Hulbert, A. J. (1985). An allometric comparison of the mitochondria of mammalian and reptilian tissues: the implications for the evolution of endothermy. *J. Comp. Physiol. B* **156**, 3-11.

Eppley, Z. A. and Russell, B. (1995). Perinatal changes in avian muscle: implications from ultrastructure for the development of endothermy. *J. Morphol.* **225**, 357-367.

Fongy, A., Romestaing, C., Blanc, C., Lacoste-Garanger, N., Rouanet, J.-L., Raccurt, M. and Duchamp, C. (2013). Ontogeny of muscle bioenergetics in Adelie penguin chicks (*Pygoscelis adeliae*). *Am. J. Physiol. Regul. Integr. Comp. Physiol.* **305**, R1065-R1075.

Girard, H. (1973). Arterial pressure in chick embryos. *Am. J. Physiol.* **224**, 454-460.

Grav, H. J., Borch-lohnsen, B., Dahl, H. A., Gabrielsen, G. W. and Steen, J. B. (1988). Oxidative capacity of tissues contributing to thermogenesis in eider (*Somateria mollissima*) ducklings: changes associated with hatching. *J. Comp. Physiol. B* **158**, 513-518.

Hillman, S. S. and Hedrick, M. S. (2015). A meta-analysis of *in vivo* vertebrate cardiac performance: implications for cardiovascular support in the evolution of endothermy. *J. Exp. Biol.* **218**, 1143-1150.

Hillman, S. S., Hancock, T. V. and Hedrick, M. S. (2013). A comparative meta-analysis of maximal aerobic metabolism of vertebrates: implications for respiratory and cardiovascular limits to gas exchange. *J. Comp. Physiol. B* **183**, 167-179.

Hohtola, E. (2004). Shivering thermogenesis in birds and mammals. In *Life in the Cold: Evolution, Mechanisms, Adaptation, and Application. Twelfth International Hibernation Symposium* (ed. B. M. Barnes and H. V. Carey), pp. 241-252. Number 27. Fairbanks, AK: Biological Papers of the University of Alaska.

Hulbert, A. J. and Else, P. L. (1989). Evolution of mammalian endothermic metabolism: mitochondrial activity and cell composition. *Am. J. Physiol.* **256**, R63-R69.

Li, F., McNelis, M. R., Lustig, K. and Gerdes, A. M. (1997). Hyperplasia and hypertrophy of chicken cardiac myocytes during posthatching development. *Am. J. Physiol. Reg. Integr. Comp. Physiol.* **273**, R518-R526.

Lopaschuk, G. D. and Jaswal, J. S. (2010). Energy metabolic phenotype of the cardiomyocytes during development, differentiation, and postnatal maturation. *J. Cardiovasc. Pharmacol.* **56**, 130-140.

Lopaschuk, G. D., Ussher, J. R., Folmes, C. D. L., Jaswal, J. S. and Stanley, W. C. (2010). Myocardial fatty acid metabolism in health and disease. *Physiol. Rev.* **90**, 207-258.

Marjoniemi, K. and Hohtola, E. (1999). Shivering thermogenesis in leg and breast muscles of galliform chicks and nestlings of the domestic pigeon. *Physiol. Biochem. Zool.* **72**, 484-492.

Moe, B., Brunvoll, S., Mork, D., Brobakk, T. E. and Bech, C. (2004). Developmental plasticity of physiology and morphology in diet-restricted European shag nestlings (*Phalacrocorax aristotelis*). *J. Exp. Biol.* **207**, 4067-4076.

Journal of Experimental Biology

Olson, J. M. (1992). Growth, the development of endothermy, and the allocation of energy in red-winged blackbirds (*Agelaius phoeniceus*) during the nestling period. *Physiol. Zool.* **65**, 124-152.

Pesta, D. and Gnaiger, E. (2012). High-resolution respirometry: OXPHOS protocols for human cells and permeabilized fibers from small biopsies of human muscle. *Methods Mol. Biol.* **810**, 25-58.

Riquelme, C. A., Magida, J. A., Harrison, B. C., Wall, C. E., Marr, T. G., Secor, S. M. and Leinwand, L. A. (2011). Fatty acids identified in the Burmese python promote beneficial cardiac growth. *Science* **334**, 528-531.

Shell, L., Burggren, W. W., Muirhead, D., Nelson, T. C. and Dzialowski, E. M. (2016). Circulatory changes associated with the closure of the ductus arteriosus in hatching emu (*Dromaius novaehollandiae*). *Comp. Biochem. Physiol. A Mol. Integr. Physiol.* **191**, 202-208.

Sirsat, T. S. and Dzialowski, E. M. (2016). Ventilation changes associated with hatching and maturation of an endothermic phenotype in the Pekin duck, *Anas platyrhynchos* domestica. *Am. J. Physiol. Regul. Integr. Comp. Physiol.* **312**, 766-775.

Sirsat, S. K. G., Sirsat, T. S., Price, E. R. and Dzialowski, E. M. (2016). Post-hatching development of mitochondrial function, organ mass, and metabolic rate in two ectotherms, the American alligator (*Alligator mississippiensis*) and the common snapping turtle (*Chelydra serpentina*). *Biol. Open* doi:10.1242/bio.017160.

Snelling, E. P., Taggart, D. A., Maloney, S. K., Farrell, A. P., Leigh, C. M., Waterhouse, L., Williams, R. and Seymour, R. S. (2015a). Scaling of left ventricle cardiomyocyte ultrastructure across development in the kangaroo *Macropus fuliginosus*. *J. Exp. Biol.* **218**, 1767-1776.

Snelling, E. P., Taggart, D. A., Maloney, S. K., Farrell, A. P. and Seymour, R. S. (2015b). Biphasic allometry of cardiac growth in the developing kangaroo *Macropus fuliginosus*. *Physiol. Biochem. Zool.* **88**, 216-225.

Starck, J. M. and Ricklefs, R. E. (1998). *Avian Growth and Development: Evolution Within the Altricial–Precocial Spectrum*. Oxford: Oxford University Press.

Steen, J. B. and Gabrielsen, G. W. (1986). Thermogenesis in newly hatched eider (*Somateria mollissima*) and long-tailed duck (*Clangula hyemails*) ducklings and barnacle goose (*Branta leucopsls*) goslings. *Polar Res.* **4**, 181-186.

Tazawa, H., Visschedijk, A. H. J., Wittmann, J. and Piiper, J. (1983). Gas exchange, blood gases and acid-base status in the chick before, during and after hatching. *Respir. Physiol.* **53**, 173-185.

Teulier, L., Rouanet, J.-L., Rey, B. and Roussel, D. (2014). Ontogeny of non-shivering thermogenesis in Muscovy ducklings (*Cairina moschata*). *Comp. Biochem. Physiol. A Mol. Integr. Physiol.* **175**, 82-89.

Walter, I. and Seebacher, F. (2009). Endothermy in birds: underlying molecular mechanisms. *J. Exp. Biol.* **212**, 2328-2336.

Whittow, G. C. and Tazawa, H. (1991). The early development of thermoregulation in birds. *Physiol. Zool.* **64**, 1371-1390.

Withers, P. C. (2001). Design, calibration and calculation for flow-through respirometry systems. *Aust. J. Zool.* **49**, 445-461.

Yeager, D. P. and Ultsch, G. R. (1989). Physiological regulation and conformation: a BASIC program for the determination of critical points. *Physiol. Zool.* **62**, 888-907.

Zhang, Y., King, M. O., Harmon, E., Eyster, K. and Swanson, D. L. (2015). Migration-induced variation of fatty acid transporters and cellular metabolic intensity in passerine birds. *J. Comp. Physiol. B* **185**, 797-810.